Perovskite Phases

Deutsche Ausgabe: DOI: 10.1002/ange.201509195
Internationale Ausgabe: DOI: 10.1002/anie.201509195

Ferromagnetism Induced by Substitution of the Iron(IV) Ion by an Unusual High-Valence Nickel(IV) Ion in Antiferromagnetic $SrFeO_3$

*Hayato Seki, Yoshiteru Hosaka, Takashi Saito, Masaichiro Mizumaki, and Yuichi Shimakawa**

Abstract: *Novel cubic perovskites $SrFe_{1-x}Ni_xO_3$ ($0 \le x \le 0.5$) with unusual high-valence iron(IV) and nickel(IV) ions were obtained by high-pressure and high-temperature synthesis. Substantial magnetic moments of Ni^{IV}, which is intrinsically nonmagnetic with a nominal d^6 electron configuration, were induced by the large magnetic moments of Fe^{IV} through orbital hybridization with oxygen. As a result, ferromagnetism with the transition temperature (T_c) above room temperature could be induced.*

In addition to the usual valence states of 3d transition-metal cations in oxides, such as Fe^{II}/Fe^{III} for Fe and Ni^{II} for Ni, unusual high-valence states, such as Fe^{IV} and Ni^{IV}, can be stabilized in a strongly oxidizing atmosphere.[1–6] Iron(IV) is stabilized in the cubic perovskite $SrFeO_3$, which is synthesized at high pressure and temperature.[2] The iron(IV) ion in the perovskite, having a nominal d^4 electron configuration in the corner-sharing FeO_6 octahedron, has a spin of $S = 2$, and at low temperatures the compound shows a helical magnetism as a result of competing ferromagnetic and antiferromagnetic interactions between the spins.[7,8] Ni^{IV}, on the other hand, is stabilized in hexagonal perovskites such as $SrNiO_3$ and $BaNiO_3$ and is expected to have a low spin state ($S = 0$).[9–11] Indeed, $BaNiO_3$ is nonmagnetic.[10,12] As reported herein, upon preparation of a solid solution of $SrFeO_3$ and $SrNiO_3$, we found that Ni^{IV} is stabilized in the $SrFeO_3$-type cubic perovskite $Sr(Fe^{IV}_{1-x}Ni^{IV}_x)O_3$ with x up to 0.5. Interestingly, the substitution of Fe^{IV} ions by Ni^{IV} ions in the helical antiferromagnetic $SrFeO_3$ induces ferromagnetism with a transition temperature (T_c) higher than room temperature.

Solid-solution samples of $Sr(Fe_{1-x}Ni_x)O_3$ were obtained by synthesis under high-pressure (10–15 GPa) and high-temperature (1273 K) conditions with $KClO_4$ as the oxidizing agent. Although very small amounts of NiO are detected in the powder X-ray diffraction (XRD) patterns, the obtained compounds with $x \le 0.5$ are found to crystalize with a cubic $Pm\bar{3}m$ perovskite structure with the general formula ABO_3 (see the XRD patterns recorded under ambient conditions in Figure S1 in the Supporting Information). As shown in Figure 1, the lattice parameter decreases linearly with increases in the amount of Ni, also confirming the successful substitution of Fe by Ni in the perovskite. Rietveld structure refinements with synchrotron XRD data confirm that the oxygen sites are fully occupied (a typical refinement result for the $x = 0.4$ compound is presented in Figure S2 and Table S1), giving the nominal composition of $Sr(Fe_{1-x}Ni_x)O_3$ with an average valence of 4+ for the B site cations.

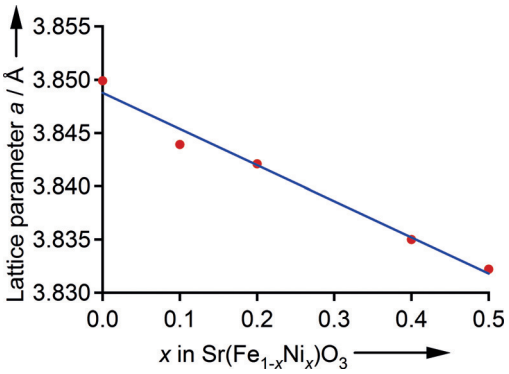

Figure 1. Composition dependence of the cubic lattice parameter of $Sr(Fe_{1-x}Ni_x)O_3$. The experimental error for each value is smaller than the size of the red data points. The blue line is a linear fit following Vegard's law.

The temperature dependence of the magnetic susceptibility of $Sr(Fe_{1-x}Ni_x)O_3$ ($0 \le x \le 0.5$) is shown Figure 2. As reported previously, $SrFeO_3$ ($x = 0$) shows an antiferromagnetic-like transition at 135 K.[7] The behaviors of the samples with $x = 0.1$ and 0.2 are similar to that of $SrFeO_3$. On the other hand, large increases in magnetization with decreasing temperature are detected for the samples with $x = 0.4$ and 0.5. Field dependence of the magnetic moment at 5 K (Figure 3) confirmed the ferromagnetic-like behaviors for the $x = 0.4$ and 0.5 samples with saturation magnetizations 2.38 and 1.80 μ_B f.u.$^{-1}$, respectively. Importantly, the magnetic transition temperatures of those samples are higher than room temperature (see Figure S3 for M–H data at room temperature).

The substitution of Fe by Ni in the antiferromagnetic $SrFeO_3$ thus induces ferromagnetism with a transition temperature higher than room temperature. If Ni^{IV} has an $S = 0$ low-spin state like that of the Ni^{IV} in $BaNiO_3$, the results suggest that the ferromagnetism is induced by introducing nonmagnetic Ni^{IV} ions into the helical antiferromagnetic Fe^{IV}

[*] H. Seki, Y. Hosaka, Prof. Dr. T. Saito, Prof. Dr. Y. Shimakawa
Institute for Chemical Research, Kyoto University
Gokasho, Uji, Kyoto 611-0011 (Japan)
E-mail: shimak@scl.kyoto-u.ac.jp
Dr. M. Mizumaki
Japan Synchrotron Radiation Research Institute, SPring-8
1-1-1 Kouto, Sayo-cho, Sayo-gun, Hyogo 679-5198 (Japan)
Dr. M. Mizumaki, Prof. Dr. Y. Shimakawa
Japan Science and Technology Agency, CREST (Japan)
Gokasho, Uji, Kyoto 611-0011 (Japan)

Supporting information for this article is available on the WWW under http://dx.doi.org/10.1002/anie.201509195.

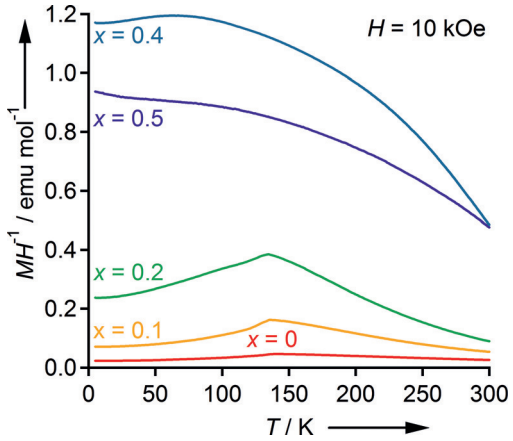

Figure 2. Temperature (T) dependence of magnetic susceptibility (MH^{-1}) for $Sr(Fe_{1-x}Ni_x)O_3$ measured at 10 kOe upon heating after zero-field cooling.

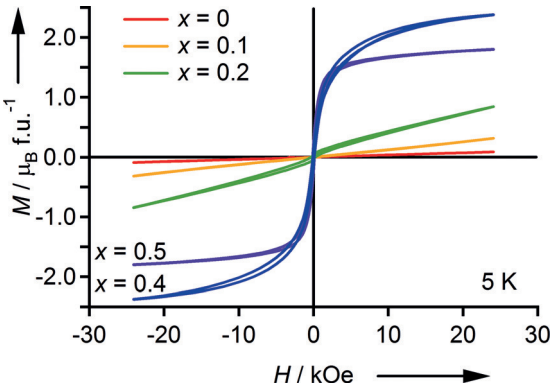

Figure 3. Magnetic field (H) dependence of magnetic moment (M) at 5 K for $Sr(Fe_{1-x}Ni_x)O_3$.

spin sublattice. To verify this hypothetical model, valence and magnetic states of cations were examined in detail. Figure 4 shows the ^{57}Fe Mössbauer spectroscopy results for $SrFe_{0.5}Ni_{0.5}O_3$ obtained at 5 and 300 K (see Table S2 for the fitting parameters). The spectrum at 5 K consists of a single component with an isomer shift (IS) of 0.090(8) mm s^{-1} relative to α-Fe and a hyperfine field (HF) of 293.8(4) kOe. These values are close to those for other Fe^{IV}-containing perovskites, such as $SrFeO_3$.[2] We can thus conclude that the valence state of the iron in the present $Sr(Fe_{1-x}Ni_x)O_3$ is kept at 4+ in the range of $0 \le x \le 0.5$. Since there is no oxygen deficiency in the perovskite structure, the results also give the unusually high-valence state of 4+ for the substituting Ni ions in the compounds. The spectrum at 300 K also confirms the ferromagnetism of the iron(IV) ions. Although the spectrum contains a Fe^{IV} paramagnetic component because the measurement temperature is close to the magnetic transition temperature, the major part, whose spectrum is considerably broadened, consists of a Fe^{IV} magnetic sextet with a reduced HF of 191.5(4) kOe.

The element selective analysis of magnetic circular dichroism (MCD) from X-ray absorption spectroscopy (XAS) reveals the magnetic structure of the ferromagnetic

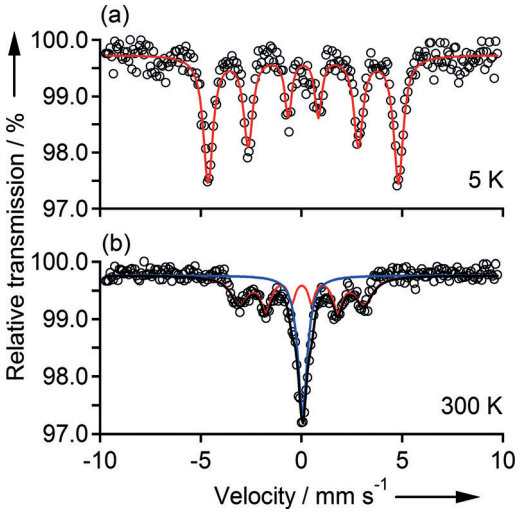

Figure 4. ^{57}Fe Mössbauer spectra of $SrFe_{0.5}Ni_{0.5}O_3$ recorded at a) 5 K and b) 300 K. The dots and solid lines, respectively, represent the measured experimental data and the Lorentzian fits.

$Sr(Fe_{1-x}Ni_x)O_3$. The XAS–MCD spectra for the $x = 0.4$ sample at 20 K, which is below the magnetic transition temperature, are shown in Figure 5. Contrary to our spec-

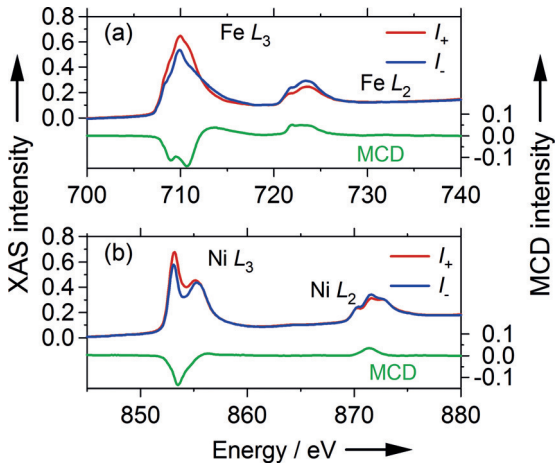

Figure 5. XAS spectra obtained using parallel (I_+; red curve) and antiparallel (I_-; blue) photon spins for $SrFe_{0.6}Ni_{0.4}O_3$ a) near the Fe L_3 and L_2 edges and b) Ni L_3 and L_2 edges. The MCD intensities, defined as the difference between the two absorption spectra, are shown at the bottom as green traces.

ulation of nonmagnetic ($S = 0$) Ni^{IV} ions, MCD intensities are evidently observed at Ni L_3 and L_2 edges, indicating the magnetic moments at the Ni^{IV} site. The MCD intensities at the L_3 and L_2 edges, respectively, for both Fe and Ni are negative and positive. The signs of the MCD intensities at the Fe L edges, being the same as the signs of the intensities at the Ni L edges, indicate that the B site Fe and Ni spins couple ferromagnetically. The spin moments obtained from the XAS–MCD intensities by using magneto-optical sum rules[13–15] are 3.69(7) μ_B for Fe and 1.26(4) μ_B for Ni. The ferromagnetic structure with those Fe and Ni spins gives the

magnetization of 2.71(5) μ_B f.u.$^{-1}$ for the sample with $x = 0.4$, which agrees well with the detected saturation moments, 2.38 μ_B f.u.$^{-1}$ at 5 K.

The magnetic structure of $SrFe_{0.6}Ni_{0.4}O_3$ was also analyzed using neutron powder diffraction data. The powder diffraction pattern at 100 K and the result of Rietveld fitting are shown in Figure 6. The refined structure parameters are listed

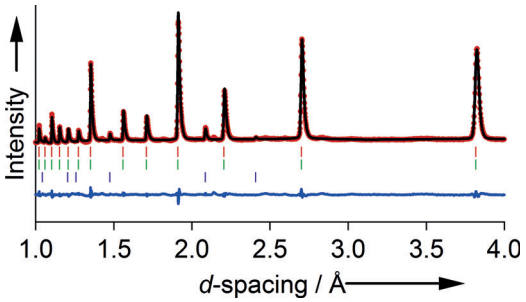

Figure 6. Neutron diffraction pattern of $SrFe_{0.6}Ni_{0.4}O_3$ at 100 K and the result of Rietveld fitting. The red dots and a black solid line represent the detected and calculated patterns, respectively. The differences between the detected and calculated intensities (shown in blue) are also plotted. Vertical marks below the profiles are Bragg reflection positions for the crystal (red) and magnetic (green) structures of $SrFe_{0.6}Ni_{0.4}O_3$ and those for the NiO crystal structure (purple). A small amount NiO impurity (5.6(2) %) was included in the refinement.

in Table S3. No order of Fe and Ni ions was detected, and the refined Fe/Ni occupation ratio (0.616(2)/0.384(2)) confirmed the random distribution of those ions at the *B* site. In addition to the nuclear reflections from the $Pm\bar{3}m$ crystal structure, magnetic intensities are apparently superimposed. No additional superstructure magnetic reflections appeared, indicating that the magnetic unit cell is the same as the crystal unit cell. The magnetic structure analysis revealed the ferromagnetic arrangement of the *B* site spins and gave a refined magnetic moment of 2.60(9) μ_B, which is consistent with the spin moments obtained from the XAS–MCD and the saturation magnetization.

The above results clearly show that the Ni^{IV} ions in $Sr(Fe_{1-x}Ni_x)O_3$ have magnetic moments, contrary to the expectation of a nonmagnetic low spin state (t_{2g}^6, $S = 0$) in an octahedral crystal field. The results also demonstrate that the substitution of Fe^{IV} by Ni^{IV} in the antiferromagnetic cubic perovskite $SrFeO_3$ induces ferromagnetism with a magnetic transition temperature above room temperature. It is difficult to describe a simple electronic structure of Ni^{IV} with a nominally d^6 electron configuration, given the magnetic moment of 1.2 μ_B for Ni detected by XAS–MCD. In the present $Sr(Fe_{1-x}Ni_x)O_3$, the low-lying 3d orbitals of the unusual high-valence Fe^{IV} and Ni^{IV} ions are expected to be strongly hybridized with the oxygen 2p orbitals, producing partially filled e_g and t_{2g} orbitals for the Ni^{IV} ions. The large magnetic moment of the Fe ion thus induces the substantial moment at the Ni site through the orbital hybridization, and a double-exchange-like interaction can mediate the ferromagnetism of Fe^{IV} and Ni^{IV}. Reducing the *B*–O bond lengths by substituting the smaller Ni^{IV} ion for Fe^{IV} also facilitates the ferromagnetic interaction, as demonstrated by the ferromagnetism detected in $SrFeO_3$ under high pressure.[16]

Note here that very recently Chen et al. computed the hypothetical cubic perovskite $SrNiO_3$ by a first-principles method and found that the ground state of $SrNiO_3$ is ferromagnetic.[17] Interestingly, they claimed that the Ni^{IV} magnetic moment of 0.855–1.689 μ_B (depending on the on-site Coulomb interaction $U = 3.0$–11.0 eV) is induced. Considering a typical U value of 5.0 eV for 3d transition-metal oxides, the predicted value (1.170 μ_B) is quite comparable to the value (1.26(4) μ_B) experimentally obtained herein by the XAS–MCD measurements. Although the cubic $SrNi^{IV}O_3$ perovskite could not be synthesized and a mixture of $Sr_3Fe_2O_7$ and NiO was obtained in our present experiments, the orbital hybridization and the large on-site Coulomb interaction should play important role in inducing the ferromagnetism of the Ni^{IV} site. With the substantial magnetic moment at the Ni^{IV} site, the magnetic interactions in $Sr(Fe_{1-x}Ni_x)O_3$ are similar to those in $Sr(Fe_{1-x}Co_x)O_3$, where Co^{IV} ($t_{2g}^4e_g^1$, $S = 3$) spins mediate the ferromagnetic spin alignment in $Sr(Fe_{1-x}Co_x)O_3$.[18–23] An important difference between the present compounds $Sr(Fe_{1-x}Ni_x)O_3$ and the previously reported compounds $Sr(Fe_{1-x}Co_x)O_3$ is that Ni^{IV} with the oxygen octahedral coordination is intrinsically nonmagnetic and that the magnetic moments of Ni^{IV} are induced by the near-neighbor Fe^{IV} magnetic moments through strong orbital hybridization. Note that the unusual high-valence states of Fe^{IV} and Ni^{IV} remain down to low temperature and no anomalies resulting from charge disproportionation and charge transfer between Fe and Ni ions were detected. As evidenced from the diffraction data, it is clear that the cubic symmetry is maintained for the samples with $x \le 0.5$. This cubic symmetry renders the *B*–O–*B* bonds linear, holding the broad conduction bands in the electronic structure, and making the metallic state stable.

In conclusion, novel cubic perovskites $Sr(Fe_{1-x}Ni_x)O_3$ with unusual high-valence Fe^{IV} and Ni^{IV} ions were obtained up to $x = 0.5$ by high-pressure and high-temperature synthesis. Substantial magnetic moments of the Ni^{IV} ion, which is intrinsically nonmagnetic with a nominal d^6 ($S = 0$) electron configuration, were induced by the large magnetic moments of Fe^{IV} through orbital hybridization with oxygen. As a result of this orbital hybridization, ferromagnetism, with the transition temperature above room temperature, was achieved.

Experimental Section

Solid solutions of $Sr(Fe_{1-x}Ni_x)O_3$ with $x = 0$, 0.1, 0.2, 0.4, and 0.5 were prepared by means of solid-state reactions. Stoichiometric amounts of Fe_2O_3 and NiO were mixed, ground in a ball mill, and calcined at 1273 K for 24 h in air. The obtained powders were then mixed with an appropriate amount of SrO_2 (stored under an argon atmosphere) and the oxidizing agent $KClO_4$ (25 wt %), sealed in platinum capsules, and treated at 1273 K and either 10 GPa ($x = 0$, 0.1, and 0.2) with a DIA-type cubic anvil press or 15 GPa ($x = 0.4$ and 0.5) with a 6–8 Kawai-type high-pressure apparatus. Attempts to prepare compounds with $x \ge 0.6$ were unsuccessful because of a solid solubility limit for Ni in cubic $SrFeO_3$. After the reaction, the residual $KClO_4$ and KCl were removed by washing in turn with distilled water and acetone.

The obtained phases and the crystal structures were analyzed by XRD with a Bruker D8 ADVANCE diffractometer and synchrotron XRD. The room-temperature synchrotron XRD patterns produced at a wavelength of 0.77425 Å were collected with a large Debye–Scherrer camera with an image plate at beamline BL02B2 in SPring-8. Each sample was packed into a glass capillary (0.1 mm in diameter) that was rotated during the measurement. The obtained diffraction data were analyzed by the Rietveld method using the program RIETAN-FP.[24] Magnetic properties of the samples were measured using a SQUID magnetometer (MPMS, Quantum Design). The sample was held in a nonmagnetic polypropylene straw and the diamagnetic signal from the holder was negligibly small. Temperature dependence of magnetic susceptibility was measured in a magnetic field of 10 kOe upon heating after cooling in a zero field. Field dependence of the magnetization was measured at several temperatures under fields ranging from −24 to 24 kOe. As a large ferromagnetic response was detected in the present experiment, the intrinsic core diamagnetic contribution was not corrected.

The ^{57}Fe Mössbauer spectrum at 5 K was obtained using a ^{57}Co/Rh radiation source. The velocity scale and the IS were determined by using pure iron metal. The spectrum was fitted with Lorentzian functions by a least-squares method. MCD spectra were obtained by a total electron yield method in XAS experiments conducted at beamline BL25SU in SPring-8. The powder sample was pasted uniformly on a sample holder by using carbon tape. The spectra at 20 K were obtained using parallel (I_+) and antiparallel (I_-) photon spins along the magnetization direction of the sample. A magnetic field of 19 kOe was applied during the measurement. The boundaries between L_3 and L_2 edges for Fe and Ni were set to 719 and 862 eV, respectively, and the MCD intensity was defined as the difference between the two absorption spectra ($I_{MCD} = I_- - I_+$). The numbers of holes for Fe and Ni were set to 6 and 4, respectively. The neutron diffraction experiments for the magnetic structure analysis were performed, with the time-of-flight method, at beamline WISH of ISIS at RAL. The data were analyzed with the FullProf program.[25]

Acknowledgements

This study was supported by Grants-in-Aid for Scientific Research (numbers 22740227 and 24540346), by a grant for the Joint Project of Chemical Synthesis Core Research Institutions from MEXT, and by the JST-CREST program of Japan. The synchrotron radiation experiments at SPring-8 were performed with the approval of the Japan synchrotron Radiation Research Institute (proposal numbers: 2015A1016). The neutron diffraction experiments were performed at beamline WISH of ISIS at RAL (UK).

Keywords: high-pressure chemistry · iron · magnetic properties · nickel · perovskite phases

How to cite: *Angew. Chem. Int. Ed.* **2016**, *55*, 1360–1363
Angew. Chem. **2016**, *128*, 1382–1385

[1] J. J. Lander, *Acta Crystallogr.* **1951**, *4*, 148–156.
[2] P. K. Gallagher, J. B. MacChesney, D. N. E. Buchanan, *J. Chem. Phys.* **1964**, *41*, 2429–2434.
[3] F. Kanamaru, H. Miyamoto, Y. Mimura, M. Koizumi, M. Shimada, S. Kume, S. Shin, *Mater. Res. Bull.* **1970**, *5*, 257–261.
[4] I. Yamada, K. Takata, N. Hayashi, S. Shinohara, M. Azuma, S. Mori, S. Muranaka, Y. Shimakawa, M. Takano, *Angew. Chem. Int. Ed.* **2008**, *47*, 7032–7035; *Angew. Chem.* **2008**, *120*, 7140–7143.
[5] Y. W. Long, N. Hayashi, T. Saito, M. Azuma, S. Muranaka, Y. Shimakawa, *Nature* **2009**, *458*, 60–63.
[6] N. Hayashi, T. Yamamoto, H. Kageyama, M. Nishi, Y. Watanabe, T. Kawakami, Y. Matsushita, A. Fujimori, M. Takano, *Angew. Chem. Int. Ed.* **2011**, *50*, 12547–12550; *Angew. Chem.* **2011**, *123*, 12755–12758.
[7] T. Takeda, Y. Yamaguchi, H. Watanabe, *J. Phys. Soc. Jpn.* **1972**, *33*, 967–969.
[8] T. Takeda, S. Komura, N. Watanabe, Ferries, Proceedings of the Third International Conference of Ferries (ICF3), Tokyo, **1980**, pp. 385–388.
[9] Y. Takeda, T. Hashino, H. Miyamoto, F. Kanamaru, S. Kume, M. Koizumi, *J. Inorg. Nucl. Chem.* **1972**, *34*, 1599–1601.
[10] H. Krischner, K. Torkar, B. O. Kolbesen, *J. Solid State Chem.* **1971**, *3*, 349–357.
[11] M. Zinkevich, *J. Solid State Chem.* **2005**, *178*, 2818–2824.
[12] R. Gottschall, R. Schöllhorn, M. Muhler, N. Jansen, D. Walcher, P. Gütlich, *Inorg. Chem.* **1998**, *37*, 1513–1518.
[13] P. Carra, B. T. Thole, M. Altarelli, X. Wang, *Phys. Rev. Lett.* **1993**, *70*, 694–697.
[14] B. T. Thole, P. Carra, F. Sette, G. van der Laan, *Phys. Rev. Lett.* **1992**, *68*, 1943–1946.
[15] Y. Teramura, A. Tanaka, T. Jo, *J. Phys. Soc. Jpn.* **1996**, *65*, 1053–1055.
[16] T. Kawakami, S. Nasu, *J. Phys. Condens. Matter* **2005**, *17*, S789–S793.
[17] G. Chen, C. Dai, C. Ma, Proceedings of the International Conference on Mechatronics, Industrial and Control Engineering (MEIC 2014), 2014, pp. 746–749.
[18] T. Takeda, S. Komura, H. Fujii, *J. Magn. Magn. Mater.* **1983**, *31-4*, 797–798.
[19] S. M. Jaya, R. Jagadish, R. S. Rao, R. Asokamani, *Phys. Rev. B* **1991**, *43*, 13274–13279.
[20] E. Smargiassi, P. A. Madden, *Phys. Rev. B* **1995**, *51*, 117–128.
[21] S. Kawasaki, M. Takano, Y. Takeda, *J. Solid State Chem.* **1996**, *121*, 174–180.
[22] J. Okamoto, K. Mamiya, S. Fujimori, T. Okane, Y. Saitoh, Y. Muramatsu, K. Yoshii, A. Fujimori, A. Tanaka, M. Abbate, et al., *Phys. Rev. B* **2005**, *71*, 104401.
[23] Y. W. Long, Y. Kaneko, S. Ishiwata, Y. Tokunaga, T. Matsuda, H. Wadati, Y. Tanaka, S. Shin, Y. Tokura, Y. Taguchi, *Phys. Rev. B* **2012**, *86*, 064436.
[24] F. Izumi, K. Momma, *Solid State Phenom.* **2007**, *130*, 15–20.
[25] J. Rodríguez-Carvajal, *Phys. B* **1993**, *192*, 55–69.

Received: October 1, 2015
Revised: November 13, 2015
Published online: December 14, 2015

